ChemComm

COMMUNICATION

View Article Online
View Journal | View Issue

Cite this: *Chem. Commun.*, 2025, **61**, 5774

Received 13th November 2024,
Accepted 14th March 2025

DOI: 10.1039/d4cc05968a

rsc.li/chemcomm

Design and synthesis of a clickable cell-permeable pseudopeptide Pin1 inhibitor with antiproliferative effects on human multiple myeloma cell line†

Lorenzo Meneghelli,[ab] Stephanie Davidson,[c] Anthony Gineste,[ab] Lamia El Guermah,[d] Sabrina Kellouche-Gaillard,[d] Franck Carreiras,[d] Ludovic Carlier,[c] Simon Nadal,[ab] Maud Larregola,[abc] Julien Pytkowicz[ab] and Chiara Zanato *[ab]

The synthesis of a library of minimal-backbone, cell-permeable, clickable pseudopeptide Pin1 ligands with potential applications in drug development and biochemical studies is reported. The ligands' affinity constants were evaluated using NMR. The lead compound 4b, demonstrated effective cell permeability, inhibitory activity, and an antiproliferative effect on a multiple myeloma cell line.

Peptidyl-prolyl isomerase NIMA-interacting-1 (Pin1), belonging to the PPIases family, catalyses the isomerization of pSer/pThr-Pro amide ω-bonds in proteins.[1] Pin1, made of two domains (WW and PPIase) linked by a flexible region, selectively targets pSer/pThr-Pro motifs in substrates, thereby influencing their regulation by kinases and phosphatases.[2] Pin1 is often overexpressed in cancers, making its inhibition a promising therapeutic strategy.[3] However, developing effective inhibitors has proven challenging due to Pin1's shallow enzymatic pocket, which limits drugability. Existing Pin1 inhibitors face several challenges, such as low potency, selectivity, and cell permeability.[4] Small molecule inhibitors lack specificity, while peptide-based inhibitors, though selective, suffer from poor permeability and metabolic instability. Although irreversible covalent inhibitors are promising,[5] they raise off-target effect concerns in long-term studies. To tackle these challenges, there is a strong interest in developing cell-permeable peptide inhibitors for Pin1. Traditional strategies, such using cyclic peptides with multiple arginine residues[6] or adding cell-penetrating peptides,[7] complicate the synthesis and modify the inhibitor scaffold. An alternative approach involves prodrugs that mask the phosphate group to enhance cell penetration and convert it to the active form within cells.[8] This strategy has seen limited use in Pin1 inhibitor development, with only two known examples. The first example served as a proof of concept for applying the "ProTide" approach to a non-sugar molecule.[9] The second example featured a conformationally locked Pin1 ligand equipped with a bis-pivaloyloxymethyl (POM) group and demonstrates the prodrug strategy's potential. However, synthesising the prodrug proved challenging.[10]

Building on these insights, we synthesised a small library of pseudopeptide Pin1 ligands with a bis-SATE (*S*-acyl-2-thioethyl) prodrug moiety.[11] Compared to bis(POM), bis(SATE) exhibited enhanced chemical and enzymatic stability.[12] The presented Pin1 ligands are also "clickable", thanks to an alkyne moiety, making them amenable to CuAACs. While no "clickable" Pin1 ligands have been reported to date, this modification could enable conjugation with azide-functionalised fluorophores, for *in vitro* imaging and permeability studies.[13] Additionally, it could facilitate the development of novel bidentate Pin1 inhibitors with enhanced binding affinity[14] or degraders (PROTACs).[15] After synthesis, ligands' K_D were evaluated, and the most promising one was tested for cell permeability, inhibitory and antiproliferative activity on ovarian adenocarcinoma (SKOV3, IGROV1) and multiple myeloma (MM1.R) cell lines.

Inspired by Etzkorn's work[16] (**1a–1b**, Fig. 1A) and the crystal structures of peptide inhibitors in Pin1 catalytic pocket,[17] the general scaffold of our Pin1 ligands comprises a minimal peptide backbone incorporating Pin1's preferences for C-terminal aromatic amino acids and N-terminal aromatic group (Fig. 1B). The Ser-Pro amide bond, which was reduced in previous work,[16] was retained to study its impact on affinity. The SATE moiety, which masks the phosphoric group to enhance cell permeability, was also included. Based on this design, three series of Pin1 ligands were synthesised (Fig. 1C). The reference ligands (**2a–2b**), developed for direct comparison with the Etzkorn's ligands and the C- and N-terminal alkyne series (**3a–3d** and **4a–4f**), designed to assess the impact of the position of the alkyne on binding affinity. The free phosphoric group versions of the ligands were also synthesised to determine the K_D in an NMR cell-free assay. Two "PseudoFmoc" (ΨFmoc) analogues (derived from the 9*H*-fluoren-9-yl-acetic acid) were also made to align with Pin1's ligand scaffold preferences while improving metabolic stability. The synthesis of **2a–b** is

[a] *BioCIS, UMR 8076, CY Cergy Paris Université, CNRS, 95000 Cergy Pontoise, France. E-mail: chiara.zanato@cyu.fr*
[b] *BioCIS, UMR 8076, Université Paris-Saclay, CNRS, Orsay, France*
[c] *CPCV, UMR 8228, Sorbonne Université, ENS, PSL, CNRS, 75005 Paris, France*
[d] *ERRMECe, MECuP, I-MAT, CY Cergy Paris Université, Cergy, 95000, France*

† Electronic supplementary information (ESI) available. See DOI: https://doi.org/10.1039/d4cc05968a

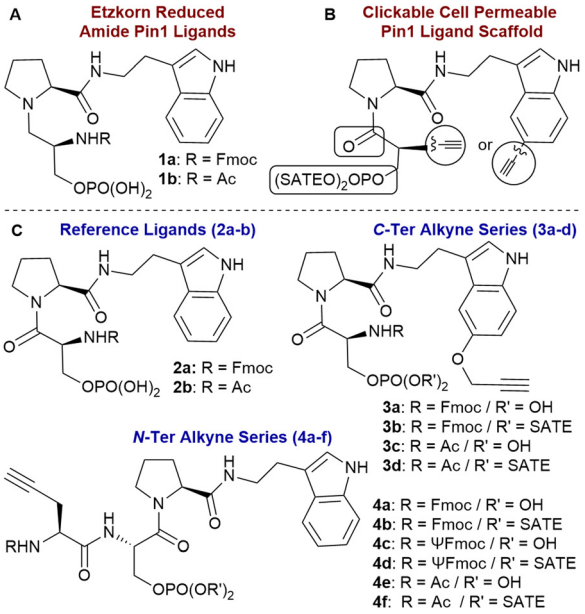

Fig. 1 (A) Etzkorn's Pin1 ligands. (B) General scaffold of presented Pin1 ligands. (C) Synthesised Pin1 ligands. (SATE: *S*-acyl-2-thioethyl, ΨFmoc: 9*H*-fluoren-9-yl-acetic acid derivative).

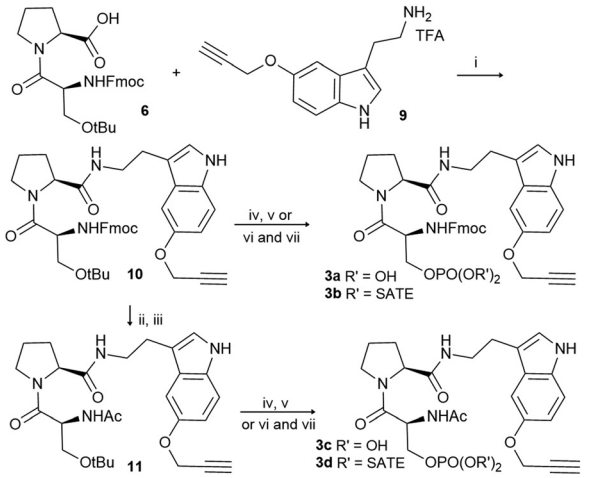

Scheme 2 Synthesis of C-terminal alkyne series. Exp. conditions: (i) DMAP, EDC, HOBt (80%); (ii) 20% DEA/DCM (80%); (iii) Ac_2O (96%); (iv) HCl 4N in dioxane (76% Fmoc-series, 71% Ac-series); (v) $P(OSATE)_2N(iPr)_2$, ETT then *t*BuOOH (80% for **3b**, 43% for **3d** or 90% for **3b**, 90% for **3d** based on recovered SM); (vi) $P(OtBu)_2N(iPr)_2$, ETT then *t*BuOOH (79% Fmoc-series, 45% Ac-series or 90% for Fmoc-series, 89% for Ac-series based on recovered SM); (vii) 20% TFA/DCM (62% for **3a**, 65% for **3c**).

shown in Scheme 1. The Fmoc-Ser(*t*Bu)-OH (**5**) reacted with H-Pro-OBn to yield, after debenzylation, peptide **6**. Coupling with tryptamine provided compound **7**, and deprotection/phosphorylation gave **2a**. For the acetylated analogue **2b**, the deprotection of **7** and acetylation of the amine is followed by *t*Bu deprotection and phosphorylation. Phosphorylation posed challenges, but phosphitylation using *N*,*N*-phosphoramidite and 5-ethylthio-*H*-tetrazole (ETT), followed by oxidation with *t*BuOOH[18] provided decent yields allowing the recycling of the unreacted alcohol. The synthetic pathway for the C-terminal alkynes **3a–d** is reported in Scheme 2. The intermediate **6** was debenzylated and coupled with **9** to give

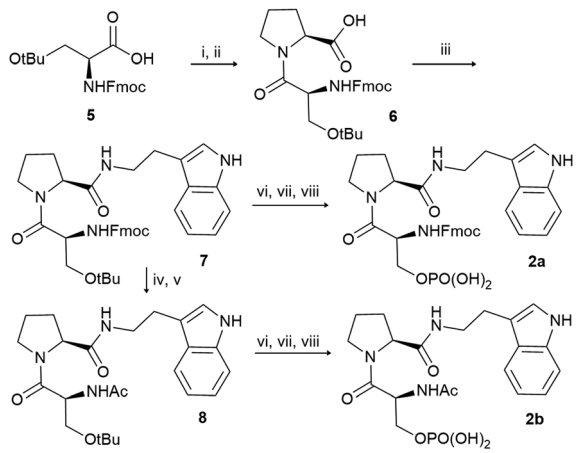

Scheme 1 Synthesis of Reference Ligands. Exp. conditions: (i) H-Pro-OBn·HCl, DIPEA, EDC, HOBt (97%); (ii) H_2, Pd/C; (iii) Tryptamine, DMAP, EDC, HOBt (93%); (iv) 20% Pip/DMF (70%); (v) Ac_2O (96%); (vi) HCl 4N dioxane (75% Fmoc-series, 80% Ac-series); (vii) $P(OtBu)_2N(iPr)_2$, ETT, THF/DCM then *t*BuOOH (45% or 90% based on recovered SM, Fmoc-series, 50% or 95% based on recovered SM, Ac series); (viii) 20% TFA/DCM (62% for **2a**, 60% for **2b**).

pseudopeptide **10**. After the acidic deprotection of the *t*Bu group, a subsequent phosphitylation followed by oxidation and deprotection provided **3a**. The bis-SATE-phosphoramidite[12] was employed to obtain **3b** with an excellent yield. The insertion of other masking groups on the OH derivative of **10** was also investigated.

The reaction with a bis-pivaloxymethyl phosphoryl chloride, to make a bis-(POM) derivative[19] provided only traces of desired compound (yields $< 2\%$). Mixed phosphoramidates derived from L-alanine methyl-ester and phenyl dichlorophosphate[20] gave no product and the starting material was recovered unreacted. The Ac analogues **3c–3d** were synthesised deprotecting **10** and acetylating the resulting amine before the *t*Bu deprotection and the phosphitylation/oxidation step. The synthesis of the N-terminal alkynes **4a–f** is reported in Scheme 3. The intermediate **7** was deprotected and coupled with Fmoc-propargylglycine to obtain **12**, which was subsequently deprotected and phosphorylated to obtain final pseudopeptides **4a** and **4b**. Compound **12** was also deprotected at N-terminus and reacted, respectively, with the 2-(9*H*-fluoren-9-yl)acetic acid to obtain **14**, or with acetic anhydride to give **15**. **4c–4f** were then obtained following the similar route of their already described analogues. To determine if the Ser-Pro amide bond or the alkyne moiety affected the binding affinity, we estimated the K_D of all synthesised ligands using the Chemical Shift Perturbations (CSPs) NMR method.[21] The backbone and $^{13}C\beta$ chemical shifts of apo Pin1 in phosphate buffer (pH 7) were previously published.[22] We confirmed the assignment of 144 out of 155 non-proline residues using 3D NMR experiments recorded on ^{15}N- and $^{15}N/^{13}C$ uniformly labelled Pin1 samples. Ligand interactions were monitored by ^{1}H–^{15}N HSQC during titrations of ^{15}N-labeled Pin1 with ligands. K_D were determined from CSPs and used to estimate the binding affinity for the WW and PPIase domains (Table 1). Reference ligand **1b** displayed a micromolar K_D (15 ± 4 μM), consistent with its reported IC_{50} (12 ± 2 μM),[22] showing selective

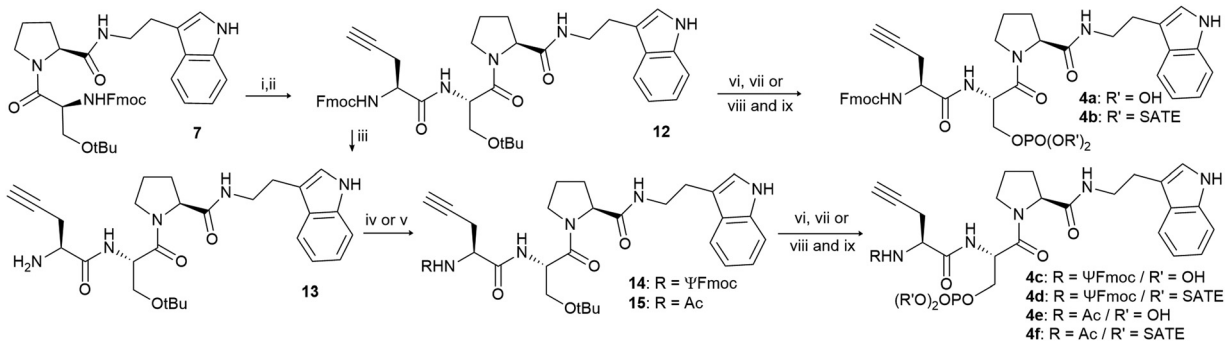

Scheme 3 Synthesis of N-terminal alkyne series. Exp. conditions: (i) 20% DEA/DCM (92%); (ii) Fmoc-Pra-OH, DMAP, EDC, HOBt (88%); (iii) 20% DEA/DCM, (95%); (iv) 2-(9*H*-fluoren-9-yl)acetic acid, DMAP, EDC, HOBt (85%); (v) Ac_2O (98%); (vi) 30% TFA/DCM, TIPS, H_2O (97% Fmoc-series, 98% Ac-series, 80% ΨFmoc-series); (vii) $P(OSATE)_2N(iPr)_2$, ETT then *t*BuOOH (45% for **4b**, 20% for **4d**, 35% for **4f** or 90% for **4b**, 80% for **4d**, 81% for **4f** based on recovered SM); (viii) $P(OtBu)_2N(iPr)_2$, ETT then *t*BuOOH (79% Fmoc-series, 50% Ac-series, 16% ΨFmoc-series or 90% Fmoc-series, 89% Ac-series, 80% ΨFmoc-series based on recovered SM); (ix) 30% TFA/DCM (20% for **4a**, 18% for **4c**, 30% for **4e**).

affinity for the PPIase domain, as supported by previously published crystal structures.[17] The non-reduced amide analogues **2a** and **2b** showed similar affinity to **1b**, indicating that the amide bond does not significantly impact Pin1 interaction intensity. However, the binding region is influenced, as both **2a** and **2b** predominantly adopt the *trans* configuration of the pSer-Pro amide bond, aligning with the WW domain's preference for *trans* conformers.[23] Compound **2a** also showed weak affinity for the PPIase domain likely due to non-specific interactions. Due to solubility issues, the affinity of **3a** could not be evaluated by NMR. Nevertheless, the introduction of an alkyne at the C-terminal seems to affect affinity, as seen with **3c**. **4a** showed significant binding to both domains and CSPs at the interdomain interface. For the WW domain, the CSPs correspond to the amino acids within the binding pocket, while no interactions were observed for those in the PPIase phosphate-binding site. This suggests that the perturbations in the PPIase domain are driven by allosteric effects. A comparison between **4a** and **2a** K_D, indicates that introducing an alkyne at the N-terminus has little impact on the binding affinity to the WW domain. NMR titration with **4c** revealed significant CSPs closely resembling those of its parent compound **4a**, both in magnitude and the affected amino acids. This indicates that both the Fmoc and the ΨFmoc groups are well tolerated. In contrast, **4e** exhibited weaker CSPs, reflecting the well-known preference of Pin1 for aromatic moieties at the N-terminal extremity. The higher affinity of **4a**, compared to other alkyne-ligands, identified its SATE version **4b** as the lead compound for the biological studies. To evaluate **4b**'s cell permeability, its fluorescent analogue, **4b-Rhod**, using Rhodamine B (Rhod) as fluorophore was synthesised (Fig. 2A). To avoid pH-dependent fluorescence,[24] Rhod was coupled with 1-(2-azidoethyl)piperazine forming a stable tertiary amide, preventing non-fluorescent spirolactam formation and ensuring consistent fluorescence at physiological pH levels for cellular imaging. Rhod was coupled *via* CuAAC, yielding the product in good yield. In contrast, conjugation of Rhod to **4b** *via* an amide bond resulted in phosphate group elimination, forming dehydroalanine. The stability of **4b-Rhod** was assessed, *via* HPLC, in two cell culture media (RPMI + 10% FBS and F12 + 10% FBS) at 37 °C over 72 hours. **4b-Rhod** showed

Table 1 K_D values obtained by NMR. Exp. conditions: 500 MHz, 298 K, 150 μM Pin1 (1 eq.) in buffer (30 mM Tris, 50 mM NaCl, 2 mM DTT), pH 7.00. A 3 mM solution of the ligand was added, from 0.1 eq. to saturation (7–8 eq.). ND: not determined – product not soluble in H_2O or buffer

Ligand	K_D WW (μM)	K_D PPIase (μM)
1b	>1000	15 ± 4
2a	26 ± 6	438 ± 80
2b	32 ± 6	>1000
3a	ND	ND
3c	439 ± 62	705 ± 302
4a	44 ± 6	88 ± 16
4c	66 ± 12	80 ± 32
4e	285 ± 32	598 ± 193

82% stability after 24 hours and 40% after 54 hours in RPMI, while only 14% remained in F12 after 30 hours, with complete degradation by 48 hours (see ESI†). These results indicate superior stability in RPMI, making it the preferred medium for further cell permeability studies. The permeability of **4b-Rhod** was evaluated in two Pin1-expressing ovarian adenocarcinoma cell lines: SKOV3, with Pin1 localised in both the cytosol and nucleus, and IGROV1, with predominantly cytoplasmic Pin1 to assess the ability of **4b-Rhod** to penetrate in different subcellular compartments. Confocal microscopy images, after 24 hours of incubation with **4b-Rhod**, were recorded (Fig. 2B). Immunofluorescence in SKOV3 cells confirmed Pin1 localisation in both the nucleus and cytoplasm, while **4b-Rhod** showed efficient cellular uptake but no nuclear penetration, likely due to SATE group cleavage in the cytoplasm. Internalization of **4b-Rhod** was also confirmed in IGROV1 cells, suggesting effective penetration in both ovarian cancer models. To confirm the cell permeability of **4b** and examine its effect on cell proliferation, an MTT viability assay was conducted at 24 and 48 hours (Fig. 2C). The multiple myeloma MM1.R cells were incubated with varying concentrations of **4b** (10, 30, and 50 μM). DMSO and untreated cells served as controls. At 10 μM, **4b** showed no significant effect on viability, consistent with the DMSO control. However, at 30 and 50 μM, **4b** caused a concentration-dependent reduction in cell proliferation. The IC_{50} of **4b** after 24 h of incubation at different concentrations (10, 25, 50, 75, 100 and 150 μM) was evaluated to be 79 ± 13 μM, aligning with

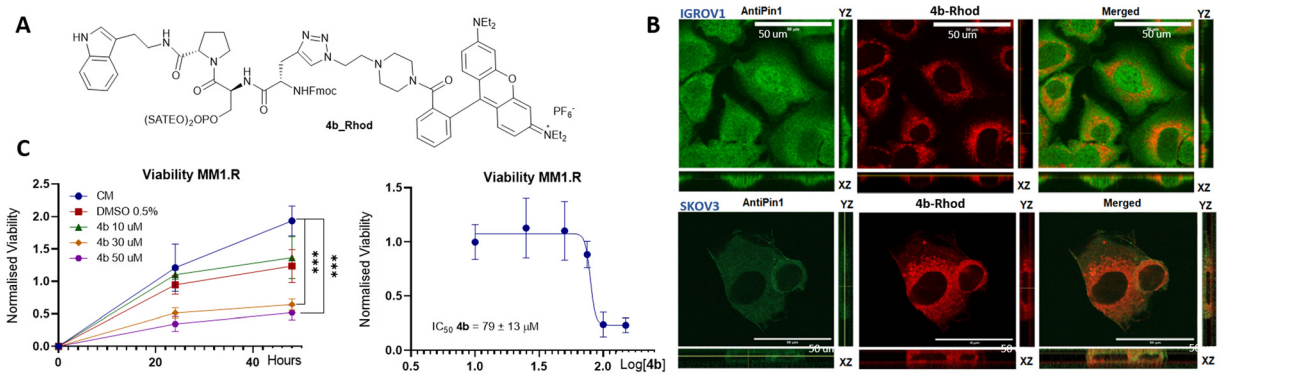

Fig. 2 (A) Chemical structure of the fluorescent probe **4b-Rhod**. (B) Microscopy Images of SKOV3 and IGROV1 cells incubated with 5 µM of **4b-Rhod** for 24 h (scale = 50 µm). (C) Cell viability assay (MTT) of MM.1R cell line after 24 h incubation with **4b**. Values are expressed as normalised viability compared with Ctrl cells in Cell Media (CM) at day 0. The data are expressed as means ± SEM; $n = 3$; *** $p < 0.0002$ (one-way ANOVA test).

its K_D (88 ± 16 µM) measured by NMR and supporting its inhibitory effect on Pin1. Given Pin1's role in cell cycle regulation, its inhibition often results in antiproliferative effects with no cytotoxicity.[5] To confirm the cell permeability of **4b**, MM1.R cells were incubated with its unprotected analogues **4a** and **4c** (see ESI†). As neither compound affected cell viability, they were considered non-permeable, supporting the conclusion that **4b**'s permeability is enhanced by the SATE group. The SensoLyte® Green Pin1 Assay was also performed (see ESI†) to evaluate **4a** and **4b** inhibition activity. **4a** minimally inhibited Pin1 at 10 µM but was effective at 100 µM. Tannic acid (Ctrl) also inhibited Pin1, while **4b** showed no inhibition due to the SATE group blocking binding.

In conclusion, this study reports the synthesis of a small library of minimal, cell-permeable, clickable pseudopeptide Pin1 ligands with K_D values determined by NMR. The lead compound **4b**, was functionalised with a fluorophore to confirm both its clickable functionality and cellular permeability. Its inhibition activity was also demonstrated. Viability assays shows **4b**'s antiproliferative activity (79 ± 13 µM) against MM1.R cells.

The ANR (*Agence Nationale de la Recherche*) is thanked for financial support (PRODIGE / ANR-21-CE07-0015) as well as CY Initiative (ANR-16-IDEX-0008). The authors thank Dr D. Sbardella for his advices in cell biology and Mr R. Besse (Cosmetomics) for technical support to the cell culture lab.

Data availability

The data supporting this article have been included as part of the ESI.† MTT Cell viability assay data have been deposited at Zenodo. Zanato C. (2024). Cell viability assay [Data set]. Zenodo. **https://doi.org/10.5281/zenodo.14034468**

Conflicts of interest

There are no conflicts to declare.

Notes and references

1 A. Matena, E. Rehic, D. Hönig, B. Kamba and P. Bayer, *J. Biol. Chem.*, 2018, **399**, 101.
2 T. Pawson and J. Scott, *Trends Biochem. Sci.*, 2005, **30**, 286.
3 Y. Nakatsu, Y. Matsunaga, K. Ueda, T. Yamamotoya, Y. Inoue, M. Inoue, Y. Mizuno, A. Kushiyama, H. Ono, M. Fujishiro, H. Ito, T. Okabe and T. Asano, *Curr. Med. Chem.*, 2020, **27**, 3314.
4 J. Moore and A. Potter, *Bioorg. Med. Chem. Lett.*, 2013, **23**, 4283.
5 B. J. Pinch, Z. M. Doctor, B. Nabet, C. M. Browne, H. S. Seo, M. L. Mohardt, S. Kozono, X. Lian, T. D. Manz, Y. Chun, S. Kibe, D. Zaidman, D. Daitchman, Z. C. Yeoh, N. E. Vangos, E. A. Geffken, L. Tan, S. B. Ficarro, N. London, J. A. Marto, S. Buratowski, S. Dhe-Paganon, X. Z. Zhou, K. P. Lu and N. S. Gray, *Nat. Chem. Biol.*, 2020, **16**, 979.
6 W. Bedewy, H. Liao, N. A. Abou-Taleb, S. F. Hammad, T. Nasr and D. Pei, *Org. Biomol. Chem.*, 2017, **15**, 4540.
7 (*a*) W. Lian, B. Jiang, Z. Qian and D. Pei, *J. Am. Chem. Soc.*, 2014, **136**, 9830; (*b*) D. Pei, *J. Med. Chem.*, 2015, **58**, 6306.
8 M. Krečmerová, P. Majer, R. Rais and B. S. Slusher, *Front. Chem.*, 2022, **10**, 1.
9 D. M. C. Schwarz, S. K. Williams, M. Dillenburg, C. R. Wagner and J. E. Gestwicki, *ACS Med. Chem. Lett.*, 2020, **11**, 1704.
10 S. Zhao and F. A. Etzkorn, *Bioorg. Med. Chem. Lett.*, 2007, **17**, 6615.
11 (*a*) F. I. Lefebvre, C. Périgaud, A. Pompon, A. M. Aubertin, J. L. Girardet, A. Kirn, G. Gosselin and J. L. Imbach, *J. Med. Chem.*, 1995, **38**, 3941; (*b*) M. Nikan, W. Li, G. A. Kinberger, P. P. Seth, E. E. Swayze and T. P. Prakash, *Molecules*, 2019, **24**, 225.
12 G. Ruda, V. P. Alibu, C. Mitsos, O. Bidet, M. Kaiser, R. Brun, M. P. Barrett and I. H. Gilbert, *ChemMedChem*, 2007, **13**, 1169.
13 Q. Jiang, X.-R. Li, C.-K. Wang, J. Cheng, C. Tan, T.-T. Cui, N.-N. Lu, T. D. James, F. Han and X. Li, *ChemComm*, 2018, **54**, 1857.
14 S. Daum, C. Lücke, D. Wildemann and C. Schiene-Fischer, *J. Mol. Biol.*, 2007, **374**, 147.
15 G. Zhong and W. Xie, *Signal Transduction Targeted Ther.*, 2024, **9**, 308.
16 G. G. Xu, Y. Zhang, A. Y. Mercedes-Camacho and F. A. Etzkorn, *Biochemistry*, 2011, **50**, 9545.
17 PDB 1PIN **https://www.rcsb.org/structure/1pin**.
18 J. W. Perich and R. B. Johns, *Tetrahedron Lett.*, 1988, **29**, 2369.
19 Y. Hwang and P. A. Cole, *Org. Lett.*, 2004, **6**, 1555.
20 C. McGuigan, J.-C. Thiery, F. Daverio, W. G. Jiang, G. Davies and M. Mason, *Bioorg. Med. Chem.*, 2005, **13**, 3219.
21 M. P. Williamson, *Prog. Nucl. Magn. Reson. Spectrosc.*, 2013, **73**, 1.
22 A. Born, P. J. Nichols, M. A. Henen, C. N. Chi, D. Strotz, P. Bayer, S.-I. Tate, J. W. Peng and B. Vögeli, *Biomol. NMR Assign.*, 2019, **13**, 85.
23 Y. M. Lee and Y.-C. Liou, *Front. Oncol.*, 2018, **8**, 469.
24 E. Birtalan, B. Rudat, D. K. Kölmel, D. Fritz, S. B. L. Vollrath, U. Schepers and S. Bräse, *Bioorg. Med. Chem. Lett.*, 2003, **13**, 2327.